Kinetic Dispersion in Redox Active Dithiocarbamate Monolayers

*Amanda L. Eckermann, Justine A. Shaw, Thomas J. Meade**

Departments of Chemistry, Biochemistry and Molecular and Cell Biology, Neurobiology and Physiology, and Radiology, Northwestern University, 2145 Sheridan Road, Evanston, IL 60208

tmeade@northwestern.edu

Supporting Information

Table of neat ferrocene dtc CV parameters.

	$E_{1/2}$	ΔE_p	FWHM	coverage
FcC11dtc	275	26	80-115	1.80E-10
FcC16dtc	264	17	80-105	2.30E-10
FcCO2C16dtc	532	9	80-90	2.50E-10

Examples of ACV i_p/i_b plots for 10, 100, 1000, and 10000 s-1Example of ACV i_p/i_b plot for a distribution of rates

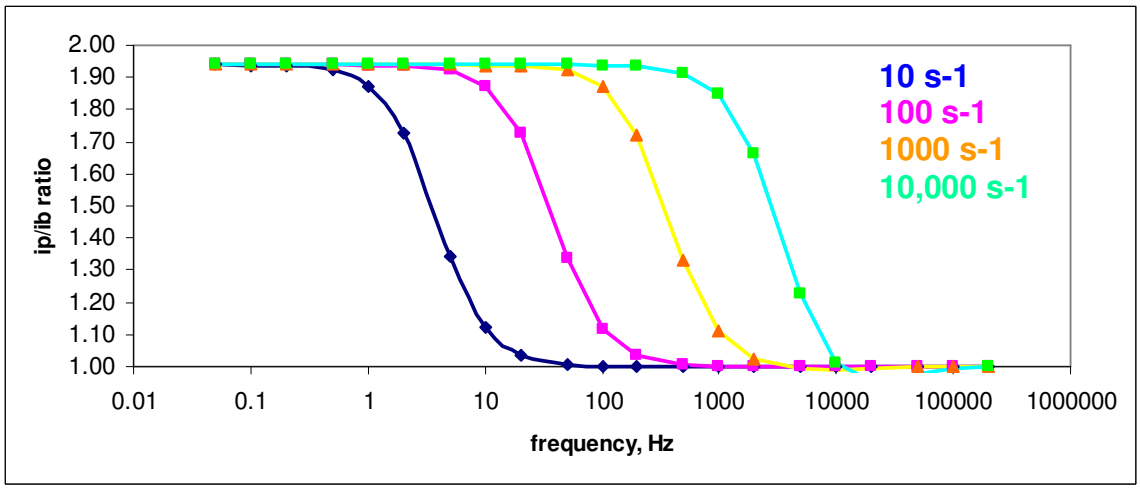

Example of ACV i_p/i_b plot for a distribution of rates (25% 10 s^{-1}; 25% 100 s^{-1}; 25% 1,000 s^{-1}, 25% 10,000s^{-1})

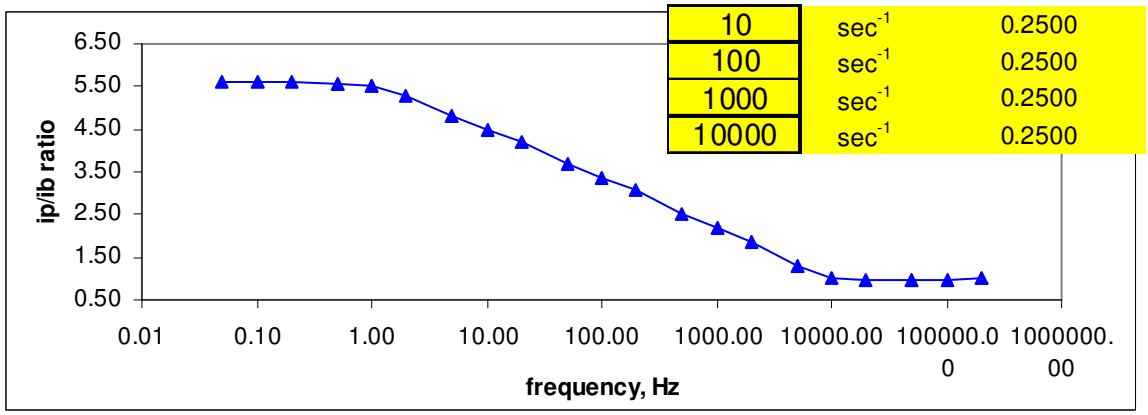

Variations within rate ranges affect the fit of the simulation to a segment of the i_p/i_b ratio plot. For example, variations of the fit within the 5,000-10,000 s^{-1} range affect the simulated i_p/i_b data at high frequencies while changes within the 1-100 s^{-1} range affect the simulated data at low frequencies.

$FcCONH(CH_2)_{15}SH$ CVs for a range of scan rates.

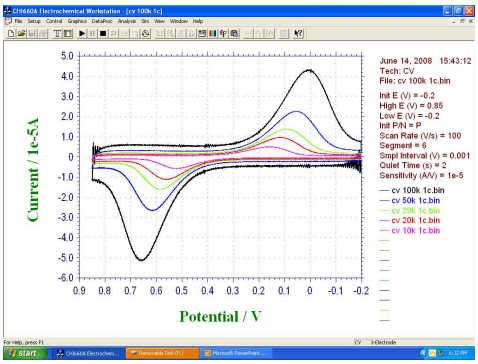

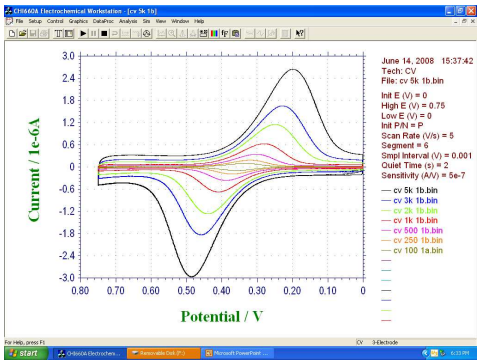

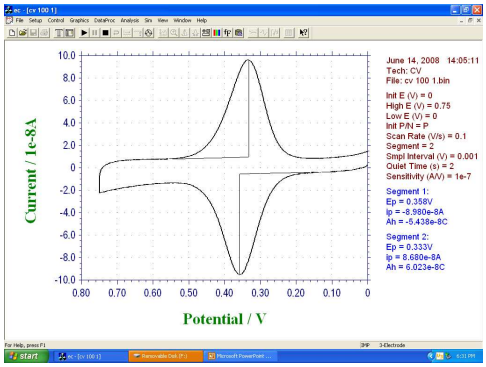

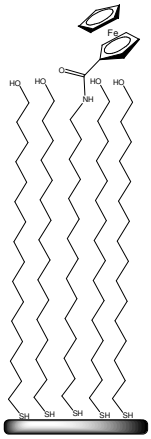

$FcCONH(CH_2)_{15}SH$ ACV ip/ib plots with fit data (experiment, red; simulation, black)

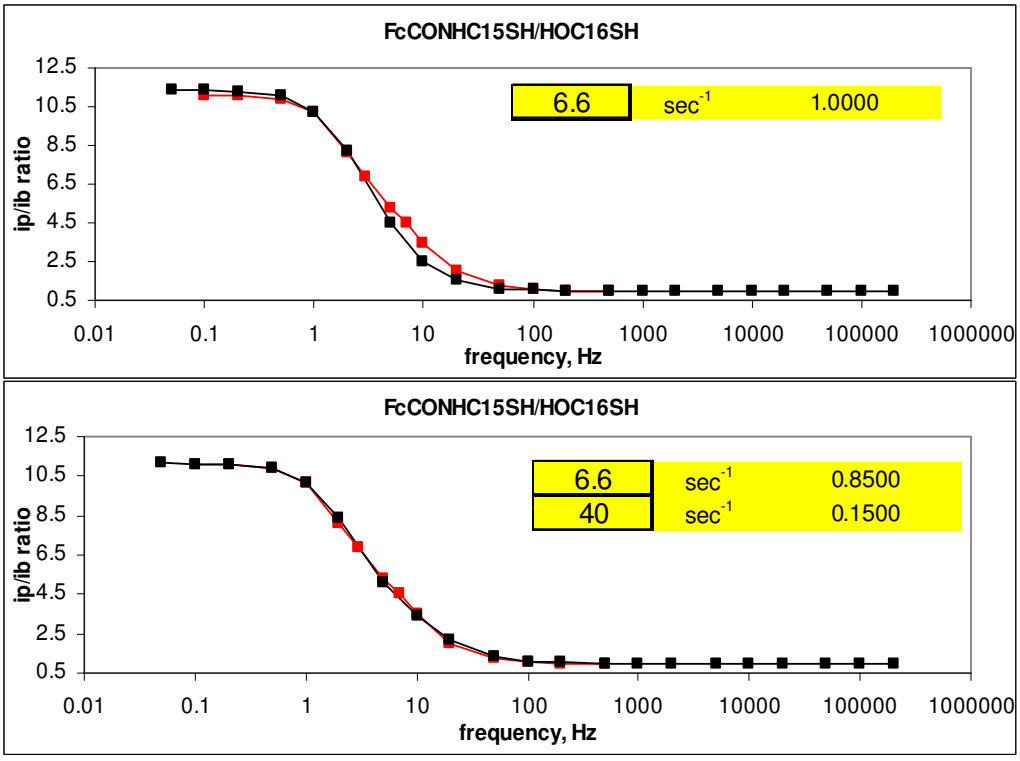

Tafel plot fit data.

For the "wide" fit, the fitting algorithm was allowed to range between 0.2-1.1eV for lambda. For the "narrow" fit, lambda was constrained to 0.8-0.9eV. The "goof" is the goodness-of-fit and a value <1 indicates a good fit.

		wide valley	wide peak	narrow valley	narrow peak
FcC16/C16	lambda(eV)	0.71	0.61	0.81	0.81
	k0 (s-1)	349	98	259	88
	coupling(eV)	3.96E-05	1.20E-05	5.97E-05	3.48E-05
	(goof)	0.68	0.63	1.19	0.89
FcC16/C18	lambda(eV)	1.01	0.91	0.98	0.92
	k0 (s-1)	0.28	0.85	0.39	0.76
	coupling(eV)	5.97E-06	5.97E-06	5.97E-06	5.97E-06
	(goof)	0.68	1.22	0.09	1.11
FcC16/CO2	lambda(eV)	0.41	0.51	0.81	0.81
	k0 (s-1)	243	996	166	259
	coupling(eV)	5.97E-06	2.15E-05	4.78E-05	5.97E-05
	(goof)	1.02	0.22	2.63	10.73

		wide valley	wide peak	narrow valley	narrow peak
FcCO2/C16	lambda(eV)	0.51	0.61	0.81	0.81
	k0 (s-1)	153	1055	111	258
	coupling(eV)	8.45E-06	3.91E-05	3.90E-05	5.97E-05
	(goof)	0.73	0.04	1.74	9.32
FcCO2/C18	lambda(eV)	0.51	0.71	0.81	0.81
	k0 (s-1)	77	762	57	258
	coupling(eV)	5.97E-06	5.85E-05	2.80E-05	5.97E-05
	(goof)	0.48	0.35	1.35	7.05
FcCO2/CO2	lambda(eV)	0.51	0.51	0.81	0.81
	k0 (s-1)	77	383	70	259
	coupling(eV)	5.97E-06	1.33E-05	3.10E-05	5.97E-05
	(goof)	1.85	0.87	2.52	1.42

Tafel plots.

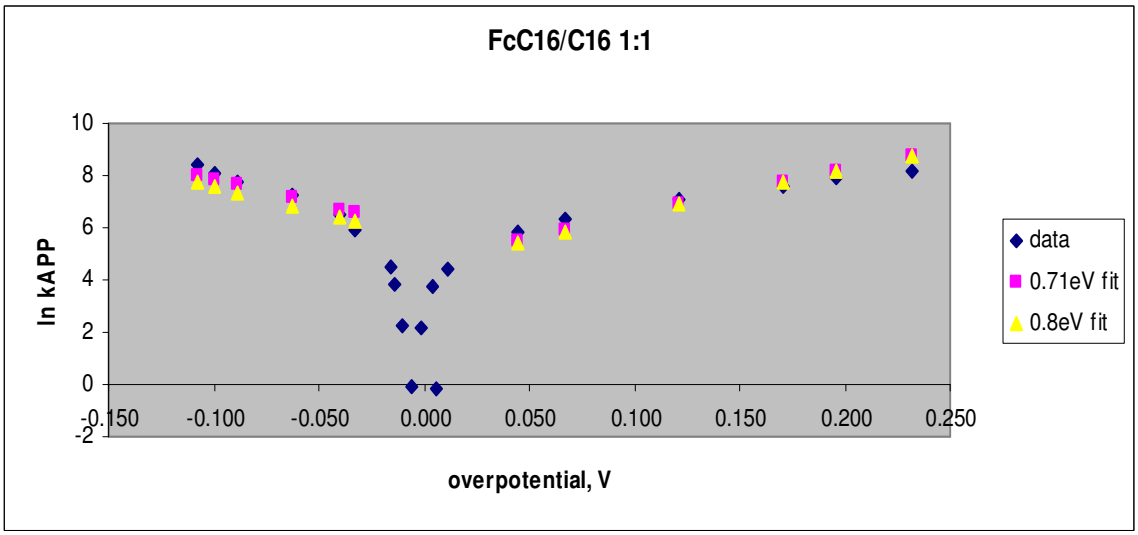
FcC16/C16 1:1
ln kAPP
overpotential, V
data
0.71eV fit
0.8eV fit

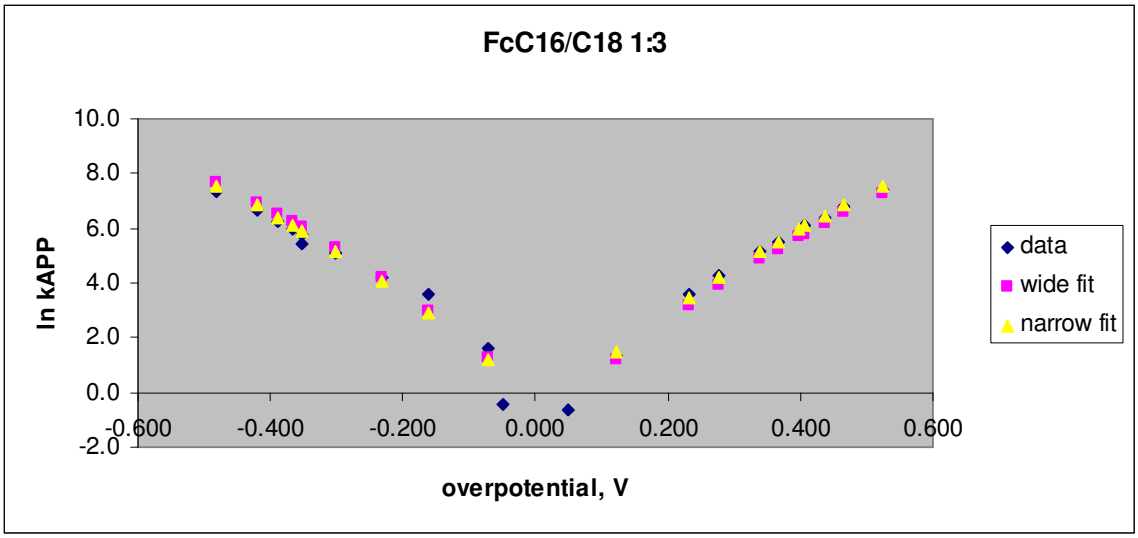
FcC16/C18 1:3
ln kAPP
overpotential, V
data
wide fit
narrow fit

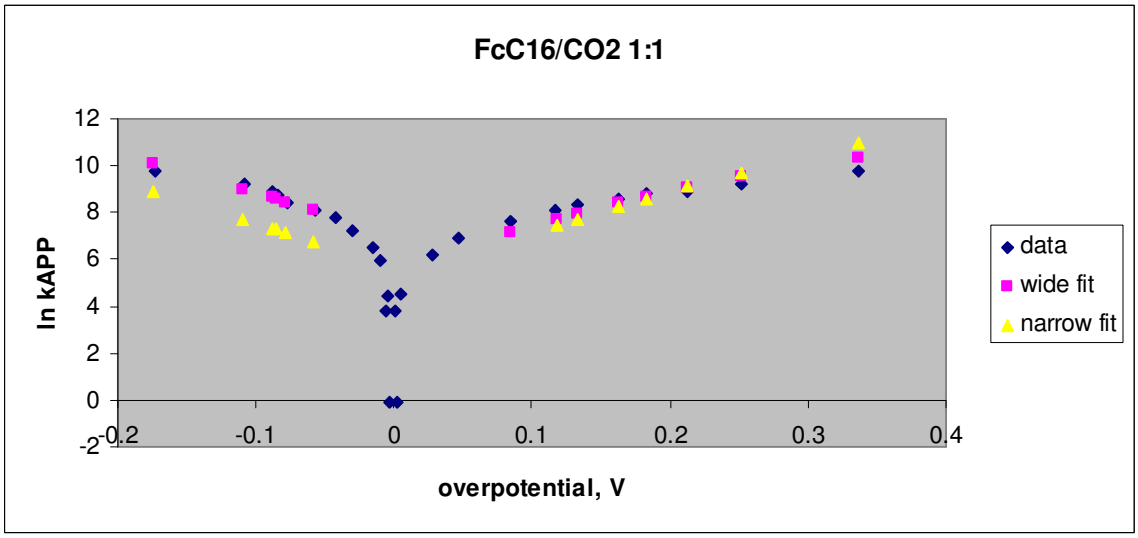
FcC16/CO2 1:1
ln kAPP
overpotential, V
data
wide fit
narrow fit

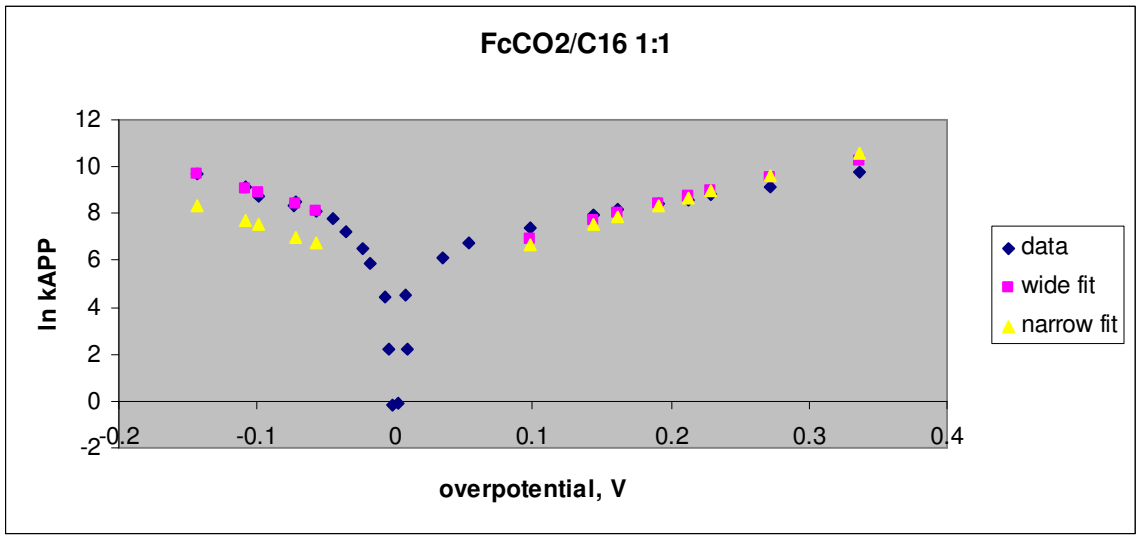
FcCO2/C16 1:1
ln kAPP
overpotential, V
data
wide fit
narrow fit

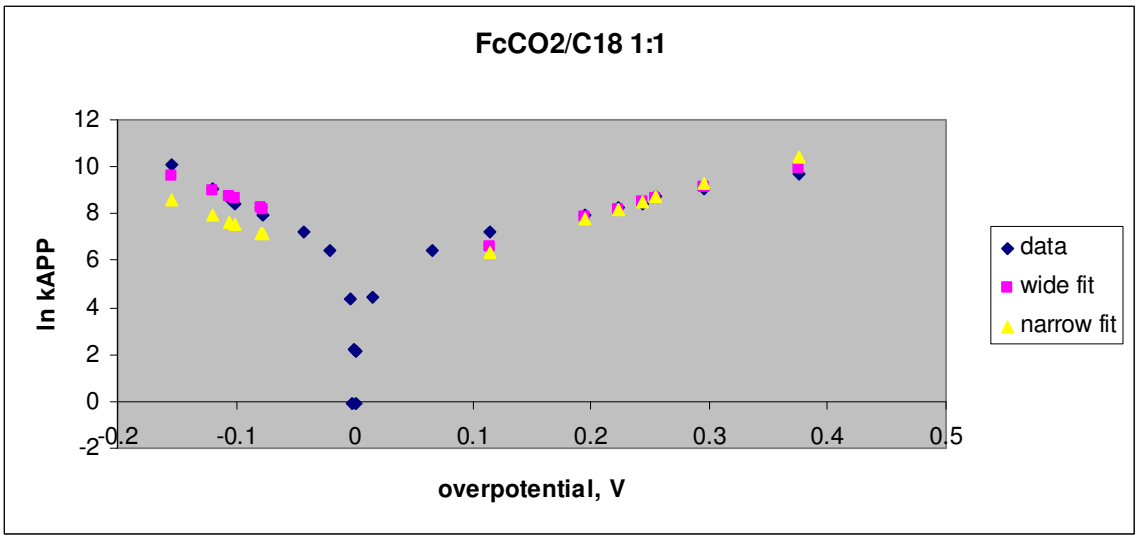
FcCO2/C18 1:1
ln kAPP
overpotential, V
data
wide fit
narrow fit

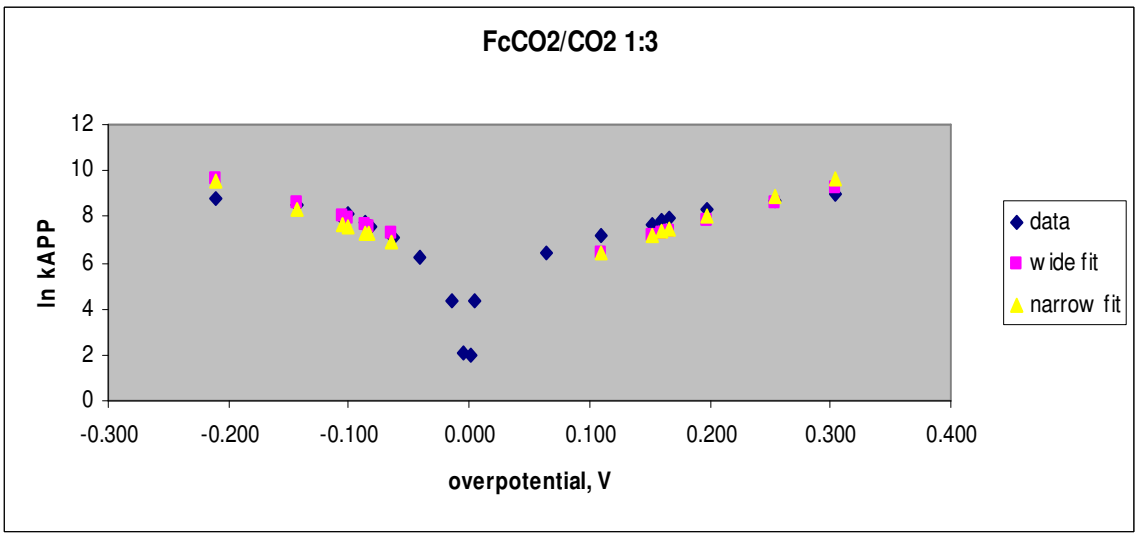
FcCO2/CO2 1:3
ln kAPP
overpotential, V
data
wide fit
narrow fit

Comparison of ACV ip/ib plots for **FcC16dtc/C16dtc** high surface coverage (1:3) and low surface coverage (1:9). The two plots can be fit to a similar distribution of rates.

1:3

rate		weight
300	sec^{-1}	0.20
1000	sec^{-1}	0.40
3000	sec^{-1}	0.15
35000	sec^{-1}	0.25

1:9

rate		weight
150	sec^{-1}	0.20
1000	sec^{-1}	0.40
2000	sec^{-1}	0.15
35000	sec^{-1}	0.25

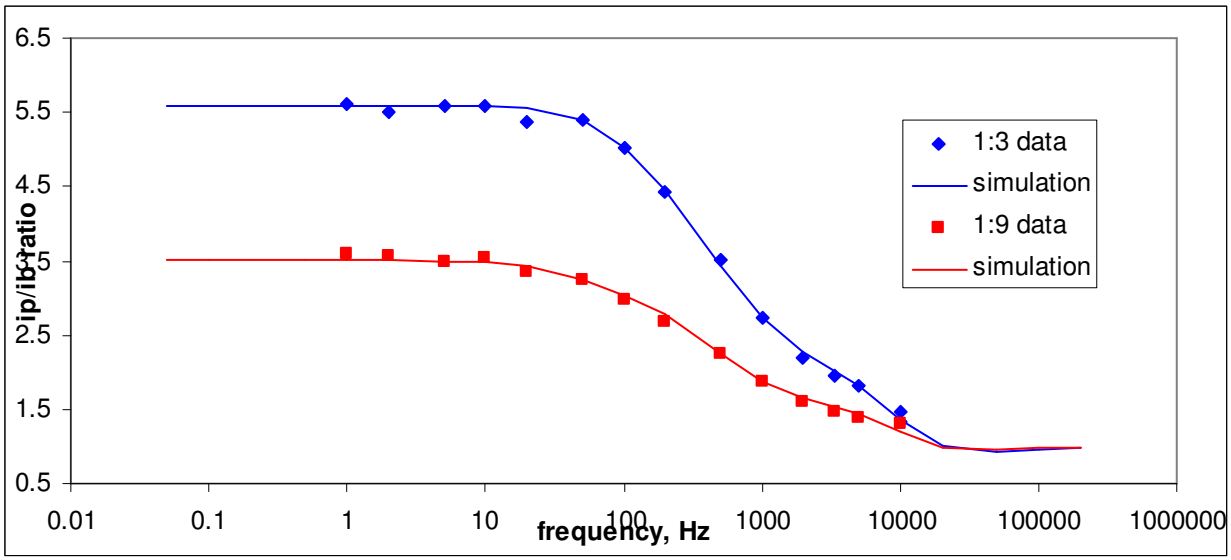

Details of Marcus density-of-states theory

Apparent cathodic and anodic rate constants are calculated as a function of overpotential for electron transfer between a redox-active molecule and a metal electrode using Marcus theory. The ET rate at a given overpotential is calculated via numerical integration of donor and acceptor levels over a range of energies ε, the energy level relative to the Fermi energy level of a metal (Equation 1).[1]

$$k_{ox} = A\int_{-\infty}^{\infty} d\varepsilon \; \mathrm{D_{ox}}(\varepsilon)\rho(\varepsilon)f(\varepsilon)$$

Equation 1

$$D_{ox}(\varepsilon) = \frac{1}{\sqrt{4\pi\lambda k_b T}}\exp\left(-\frac{(\lambda - \varepsilon + e_0\eta)^2}{4\lambda k_b T}\right)$$

Equation 2

The Fermi function $f(\varepsilon)$ of the metal gives the probability that a given available electron energy state will be occupied at a given temperature.[2] The density of states of the metal, $\rho(\varepsilon)$, is assumed to be constant over the range of energies used to evaluate the integral since the density of states varies slowly near the Fermi level.[3] The distribution of electron acceptor levels of the redox center is represented by a Gaussian function $D_{ox}(\varepsilon)$ whose widths are defined as the reorganization energy (Equation 2). The reorganization energy parameter λ can be partitioned into inner- (λ_i) and outer-sphere (λ_o) reorganization energy components. The inner-sphere component λ_i is related to the changes in bond lengths and angles that accompany the change in redox state of the redox species. An analytical expression for the outer-sphere reorganization energy of electron transfer between a redox center (approximated as a spherical cavity) and an electrode in a dielectric continuum is shown in Equation 3. In this expression for λ_o, e is the electron charge, N_A is Avogadro's number, a is the radius of the redox center, d is the distance between the redox center and the electrode, ε_s is the static dielectric constant of the solvent, and

ε_{op} is the optical frequency dielectric constant. The preintegral factor, A in Equation 1, includes factors such as electronic coupling, the probability of tunneling through an electronic barrier and surface coverage of redox active sites.

$$\lambda_O = \left(\frac{e^2 N_A}{2}\right)\left(\frac{1}{a} - \frac{1}{2d}\right)\left(\frac{1}{\varepsilon_{op}} - \frac{1}{\varepsilon_s}\right) \qquad \text{Equation 3}$$

1. Chidsey, C. E. D., *Science* **1991,** 251, (4996), 919-22.
2. Kittel, C., *Introduction to Solid State Physics*. 4th Edition; John Wiley & Sons: 1971.
3. Schmickler, W., *Interfacial Electrochemistry.* Oxford University Press: 1996.

1H NMR data and ESI-MS data

FcC11 86% ^{1}H NMR (401 MHz, $CDCl_3$) δ 4.07 (s), 4.02 (d), 2.63 (t), 2.29 (t), 1.54 (m), 1.47 (m), 1.25 (m), 0.87 (s). ESI-MS m/e Calcd 523.4 Found [M+H] 524.3 **FcC16** 53% ^{1}H NMR (500 MHz, $CDCl_3$) δ 4.08 (s), 4.04 (s), 4.02 (s), 2.65 (m), 2.30 (m), 1.57 (m), 1.48 (m), 1.25 (m), 0.88 (t). ESI-MS m/e Calcd 649.5 Found [M+H] 650.5 **FcCO2C16** 84% ^{1}H NMR (499 MHz, $CDCl_3$) δ 4.74 (s), 4.32 (s), 4.14 (m), 2.75 (s), 1.65 (m), 1.36 (m), 1.18 (m), 0.81 (t). ESI-MS m/e Calcd 693.5 Found [M+H] 694.5 **C16** 35% ^{1}H NMR (500 MHz, $CDCl_3$) 2.84 (m), 1.8 (m), 1.25 (m), 0.88 (t). ESI-MS Calcd 465.5 Found [M+] 465.2 **CO2C16** 76% ^{1}H NMR (500 MHz, $CDCl_3$) 3.67 (s), 2.59 (t), 2.30 (t), 1.49 (m), 1.25 (m), 0.88 (t). ESI-MS Calcd 532.5 Found [M+H] 533.9